Beddington–DeAngelis Functional Response, Fear Among Prey and Saturating Prey Refuge

OGBU FAMOUS IMAGA[1,2], NIKOS MASTORAKIS[2]
[1]Department of Mathematics
Covenant University
Canaanland, Ota
NIGERIA

[2]Technical University of Sofia
English Language Faculty of Engineering, Clement Ohridski 8,
Sofia 1000,
BULGARIA

Abstract: - A non-autonomous, time-periodic predator-prey system incorporating an epidemic outbreak within the prey population, a fear effect, a saturating prey refuge, horizontal disease transmission among prey, and a Beddington–DeAngelis functional response. The positivity and uniform boundedness of the population trajectories within a compact invariant region is established. By applying Mawhin's Coincidence Theorem and constructing a logarithmic coordinate transformation, sufficient conditions for the existence of at least one positive ω-periodic solution is obtained. Furthermore, by employing a global logarithmic Lyapunov functional approach, we establish criteria ensuring that this periodic solution acts as a global attractor for the ecosystem. Numerical simulations to validate the analytical results were performed. The results demonstrate that while heightened fear suppresses susceptible prey birth rates, it simultaneously dampens disease transmission, altering the geometric scale and positioning of the system's periodic attractors.

Key-Words: - Eco-epidemiology, Beddington–DeAngelis functional response, Fear effect, Saturating prey refuge, Mawhin's Coincidence Theorem, Global attractor.

Received: April 19, 2026. Revised: May 18, 2026. Accepted: June 21, 2026. Published: November 25, 2026.

1 Introduction

The complex relationships within ecosystems where infectious diseases and predator-prey interactions co-occur has been extensively studied in Mathematical biology. Early traditional predator-prey models assumed that predators affected prey populations solely through direct killing however, the authors in [1] through their field experiment showed that predators can also affect prey population pyschologically. The presence of a predator can affect the prey population by restricting the reproductive output of the avian. This phenomenon formally known as "fear effect" has prompted widespread interest in modeling how anti-predator behaviour changes population rates across different species [2], [3]. In order to appropriately represent this behavioural shift, different researchers have proposed various functional adjustments where the predator density down-regulates the prey birth rate [4]. These mathematical formulations have revealed complex bifurcations, stability switches and chaotic regimes [5], [6] that the traditional direct consumption models failed to predict, even when incorporating adaptive avoidance strategies [7] or multiple foraging mechanisms [8].

The spread of infectious diseases within wildlife communities has lead to the emergence of the field of eco-epidemiology, which combines population ecology with disease dynamics [9]. Diseases can profoundly destabilize community structures, driving cyclic oscillations or accelerating species extinction [10]. Depending on the specific biological mechanisms of the system, epidemics may infect the predator population [11], [12], spread through social predators [13], or cycle within diseased predator ecosystems governed by modified Leslie–Gower or Holling-type frameworks [14], [15], [16]. Furthermore, parasites frequently affect the behaviour of the host by increasing their vulnerability to top-tier

predators [17].

To in order to evade predation, prey populations frequently utilize structural or spatial anomalies known as prey refuges [18]. Refuges provide safety zones that isolate a portion of the prey population, effectively mitigating over-exploitation and preventing sudden ecosystem collapse [19]. Classic models exploring constant or proportional refuge allocations have shown that safety zones can damp predatory oscillations and stabilize steady states [20]. When predation pressures exhibit highly nonlinear dynamics, incorporating more realistic functional responses becomes vital. The Beddington–DeAngelis functional response addresses these complexities by integrating mutual interference among predators alongside prey saturation [21]. When combined with density-dependent delays and saturating refuge capacities, these formulations provide a highly accurate representation of real-world predator-prey dynamics [22]. Additionally, understanding these complex relationships requires analyzing higher-order interactions, such as intraguild predation where competitors actively consume one another [23].

While autonomous formulations offer valuable foundational insights [24], natural ecosystems are inherently driven by environmental fluctuations, such as seasonal weather changes, diurnal cycles, and periodic resource availability. Consequently, modeling these interactions using non-autonomous, time-periodic differential equations offers a much more rigorous and biologically realistic model. Establishing the criteria for the existence and permanence of periodic states in time-varying systems requires sophisticated analytical tools [25], [26], [27]. Researchers frequently leverage foundational results in delay equations [28] and conditions governing global attractivity in multi-species competition [29], [30]. Central to these topological derivations is Mawhin's Coincidence Theorem [31], which utilizes coincidence degree theory to prove the existence of periodic solutions in non-monotonic systems.

The existence of a positive periodic solution in an eco-epidemiological system is investigated in this study by formulating a non-autonomous, time-periodic predator-prey model. The model explicitly incorporates a fear effect, a saturating prey refuge, disease transmission among prey, and a Beddington–DeAngelis functional response.

2 Mathematical model formation

The total population of the ecosystem is divided into three distinct classes which are $A(t)$, the density of susceptible prey at time t, $B(t)$, the density of infected prey at time t, and $C(t)$, the density of predators at time t. Assuming that all biological and environmental parameters are continuous, positive, ω-periodic functions of time t (i.e., $g(t+\omega)=g(t)$), with bounds on the interval $[0,\omega]$ defined as $g^L = \min_{t\in[0,\omega]} g(t) > 0$ and $g^M = \max_{t\in[0,\omega]} g(t) > 0$. The system of differential equations is given by:

$$\begin{aligned}
\frac{dA}{dt} &= \frac{r(t)A}{1+f(t)C}\left(1-\frac{A+B}{K(t)}\right) - \frac{\beta(t)AB}{1+bB} \\
&- \frac{a_1(t)\left[A-R(t,A)\right]C}{1+b_1(t)\left[A-R(t,A)\right]+b_2(t)B+c(t)C}, \\
\frac{dB}{dt} &= \frac{\beta(t)AB}{1+bB} - d_1(t)B - \alpha(t)B \\
&- \frac{a_2(t)BC}{1+b_1(t)\left[A-R(t,A)\right]+b_2(t)B+c(t)C} \\
\frac{dC}{dt} &= -d_2(t)C \\
&+ \frac{k_1(t)a_1(t)\left[A-R(t,A)\right]C + k_2(t)a_2(t)BC}{1+b_1(t)\left[A-R(t,A)\right]+b_2(t)B+c(t)C.}
\end{aligned} \tag{1}$$

The system (1) is analyzed in the positive invariant region $\mathbb{R}^3_+$, with $A(0) > 0$, $B(0) > 0$, $C(0) > 0$ and the saturating prey refuge function $R(t,A)$ is given by $R(t,A) = \frac{m(t)A}{1+n(t)A}$. The parameter functions $g(t) \in \{r, f, K, \beta, a_1, a_2, b_1, b_2, c, d_1, d_2, \alpha, m, n, k_1, k_2\}$ are continuous, positive, and ω-periodic, $(A - R(t,A) \geq 0)$ and $0 < m(t) < 1, \quad \forall t \in [0,\omega]$. Infected prey are assumed to be too weak to use the refuge. The ecological meanings of the parameters are shown in Table 1 below

Table 1: Biological significance of parameters

Parameter	Description
$\frac{1}{1+f(t)C}$	predator induced cost of fear where $f(t)$ is the intensity of anti-predator response
$r(t), K(t)$	susceptible prey growth rate and the environmental carrying capacity
β	rate of disease transmission
$d_1(t),\ \alpha(t)$	natural death rate and disease-induced mortality rate of infected prey
$R(t,A) = \frac{m(t)A}{1+n(t)A}$	Saturating prey refuge with $m(t)$ representing the refuge capacity coefficient and $n(t)$ is the environmental scaling factor

$A - R(t, A)$	density of susceptible prey exposed to predation
$a_1(t), a_2(t)$	attack rates of predators on susceptible and infected prey respectively
$b_1(t),\ b_2(t)$	handling time coefficient for the susceptible and infected prey respectively
$c(t)$	mutual interference coefficient
$k_1(t),\ k_2(t)$	predator conversion rate for consuming susceptible and infected prey respectively
$d_2(t)$	natural death rate of the predators

Source: Created by the Authors.

In this paper, we establish sufficient conditions for the existence, uniqueness and global attractivity of the periodic solution for the system (1). The Mawhin's coincidence degree theorem is used to establish existence results. Furthermore, numerical simulation is used to validate the analytical results.

The rest of this work is orgainized as follows. Section 3 shows that the system is well-defined while in section 4, Mawhin continuation theorem is used to establish conditions for existence of periodic solution. In section 5, using a logarithm Lyapunov function the uniqueness and global attractivity of the periodic solution is studied. Finally, in section 5, the analytical results are validated using numerical simulation.

3 Positivity and Boundedness of the Model

We will confirm that the eco-epidemiological system is biologically well-behaved under the established constraints, by proving that any solution starting with positive initial conditions remains strictly positive and bounded for all future time $t \geq 0$.

3.1 Positivity

We show that the positive region $\mathbb{R}^3_+ = \{(A, B, C) \in \mathbb{R}^3 : A > 0, B > 0, C > 0\}$ is an invariant region for the system. We rewrite (1), as

$$\begin{aligned} \frac{dA}{dt} &= A(t) \cdot F_1(A, B, C, t), \\ \frac{dB}{dt} &= B(t) \cdot F_2(A, B, C, t), \\ \frac{dC}{dt} &= C(t) \cdot F_3(A, B, C, t), \end{aligned} \tag{2}$$

where

$F_1(A, B, C, t) = \frac{r(t)}{1+f(t)C}\left(1 - \frac{A+B}{K(t)}\right) - \frac{\beta(t)B}{1+bB} - \frac{a_1(t)\left[1-\frac{m(t)}{1+n(t)A}\right]C}{1+b_1(t)[A-R(t,A)]+b_2(t)B+c(t)C}$,

$F_2(A, B, C, t) = \frac{\beta(t)A}{1+bB} - d_1(t) - \alpha(t) - \frac{a_2(t)C}{1+b_1(t)[A-R(t,A)]+b_2(t)B+c(t)C}$,

$F_3(A, B, C, t) = \frac{k_1(t)a_1(t)[A-R(t,A)]+k_2(t)a_2(t)B}{1+b_1(t)[A-R(t,A)]+b_2(t)B+c(t)C} - d_2(t)$.

Solving (2), we obtain

$$\begin{aligned} A(t) &= A(0)e^{\int_0^t F_1(A(\tau),B(\tau),C(\tau),\tau)\,d\tau}, \\ B(t) &= B(0)e^{\int_0^t F_2(A(\tau),B(\tau),C(\tau),\tau)\,d\tau}, \\ C(t) &= C(0)e^{\int_0^t F_3(A(\tau),B(\tau),C(\tau),\tau)\,d\tau}. \end{aligned}$$

Since $A(0) > 0$, $B(0) > 0$, $C(0) > 0$ and the exponential function is strictly positive for any real exponent, $A(t) > 0$, $B(t) > 0$, $C(t) > 0$, for all $t \geq 0$. Therefore, the solution $(A(t), B(t), C(t))$ remains strictly inside $\mathbb{R}^3_+$ for all $t \geq 0$.

3.2 Boundedness

By applying the Comparison Theorem, we show that the populations cannot grow to infinity due to resource limitations. From (1), we have

$$\frac{d(A+B)}{dt} \leq \frac{r(t)A}{1+f(t)C}\left(1 - \frac{A+B}{K(t)}\right). \tag{3}$$

Since $1 + f(t)C > 1$, $A \leq A + B$, and the maximum bounds of our periodic parameters are r^M and K^M, (3) becomes

$$\frac{d(A+B)}{dt} \leq r^M(A+B)\left(1 - \frac{A+B}{K^M}\right). \tag{4}$$

Letting $N(t) = A(t) + B(t)$, (4) becomes the standard logistic differential inequality

$$\frac{dN}{dt} \leq r^M N\left(1 - \frac{N}{K^M}\right). \tag{5}$$

By the standard comparison theorem, we obtain

$$\limsup_{t\to\infty} N(t) \leq K^M.$$

Thus, there exists a $T_1 > 0$ such that for all $t > T_1$, $A(t) + B(t) \leq K^M + \epsilon_1$ $(\epsilon_1 > 0)$. Hence, both $A(t)$ and $B(t)$ are bounded by $Z_1 = K^M + \epsilon_1$. Next, let $W(t) = A(t) + B(t) + \frac{1}{k^L}C(t)$ where

$k^L = \min\{\inf_t k_1(t), \inf_t k_2(t)\} > 0$. Then,

$$\begin{aligned}\frac{dW}{dt} &= \frac{dA}{dt} + \frac{dB}{dt} + \frac{1}{k^L}\frac{dC}{dt}\\ &= \frac{r(t)A}{1+f(t)C}\left(1 - \frac{A+B}{K(t)}\right) - d_1(t)B\\ &\quad - \alpha(t)B - \frac{1}{k^L}d_2(t)C\\ &\quad - \frac{(a_1(t)[A - R(t,A)]C + a_2(t)BC)}{1 + b_1(t)[A - R(t,A)] + b_2(t)B + c(t)C}\\ &\quad + \frac{\frac{k_1(t)}{k_L}a_1(t)[A - R(t,A)]C}{1 + b_1(t)[A - R(t,A)] + b_2(t)B + c(t)C}\\ &\quad - \frac{\frac{k_2(t)}{k_L}a_2(t)BC}{1 + b_1(t)[A - R(t,A)] + b_2(t)B + c(t)C}.\end{aligned} \tag{6}$$

Since $\frac{k_1(t)}{k_L} \geq 1$ and $\frac{k_2(t)}{k^L} \geq 1$, the terms involving predation cancel down defensively into negative expressions. Dropping them yields a simplified differential inequality. Now, let $\delta > 0$ be a constant such that $0 < \delta < \min\{d_1^L + \alpha^L, d_2^L\}$ then (6) becomes

$$\begin{aligned}\frac{dW}{dt} + \delta W &\leq r^M A\left(1 - \frac{A}{K^M}\right) + \delta A\\ &\quad - (d_1(t) + \alpha(t) - \delta)B - \frac{1}{k^L}(d_2(t) - \delta)C\\ &\leq r^M A\left(1 - \frac{A}{K^M}\right) + \delta A\\ &\leq \frac{(r^M + \delta)^2 K^M}{4r^M} \equiv Z_2\end{aligned}$$

Applying Gronwall's Inequality, we obtain

$$W(t) \leq W(0)e^{-\delta t} + \frac{Z}{\delta}\left(1 - e^{-\delta t}\right).$$

Taking the limit superior as $t \to \infty$, we obtain $\limsup_{t\to\infty} W(t) \leq \frac{Z}{\delta}$. Since $C(t) \leq k^M W(t)$, there exists a $T_2 > T_1$ such that for all $t > T_2$, $C(t) \leq \frac{k^M Z}{\delta} + \epsilon_2 \equiv Z_3$ ($\epsilon_2 > 0$). Every positive solution $(A(t), B(t), C(t))$ of the eco-epidemiological system enters and remains confined within the bounded compact set $\Omega = \left\{(A, B, C) \in \mathbb{R}^3_+ : A + B \leq Z_1,\, C \leq Z_3\right\}$

4 Existence of Periodic Solution

In this section, we will establish conditions for the existence of periodic solutions to system (1). We will first provide some preliminary information.

Let $U : \text{Dom } U \subset X \to Y$ a linear map and $V : X \to Y$ be a continuous map where X and Y are Banach spaces. U is called a Fredholm operator of index zero if Im U is closed in Y and $\dim \ker U = codim \text{ Im } U < \infty$. For the Fredholm operator U, there exists two continuous projection $S : X \to X$ and $T : Y \to Y$ Im $S = \ker U$ and $\ker T = \text{Im } U = \text{Im } (I - T)$, thus $U|_{\text{Dom } U \cap \ker S} : (I - S)X \to \text{Im } U$ is invertible. The inverse of this map is denoted by W_S, where $W_S : \text{Im } U \to \text{Dom } U \cap \ker S$. Let $\Omega \times [0,1] \subset X$ be an open set, if $TV(\overline{\Omega} \times [0,1])$ is bounded and $W_S(I - T)T(\overline{\Omega} \times [0,1]) \subset X$ is compact, then $T(\overline{\Omega} \times [0,1]) \times [0,1]$ is L-compact. We introduce the following notations:

$$\overline{g} = \frac{1}{\omega}\int_0^\omega g(t)dt \quad g^L \min_{t\in[0,\omega]} g(t), \quad g^M \max_{t\in[0,\omega]} g(t),$$

where g is a continuous ω-periodic function.

In order to ensure that the populations remain strictly positive, we make a logarithmic coordinate transformation. Let $A(t) = e^{w_1(t)}$, $B(t) = e^{w_2(t)}$, and $C(t) = e^{w_3(t)}$, (1) becomes

$$\begin{aligned}\frac{dw_1}{dt} &= \frac{r(t)}{1+f(t)e^{w_3}}\left(1 - \frac{e^{w_1} + e^{w_2}}{K(t)}\right) - \frac{\beta(t)e^{w_2}}{1 + be^{w_2}}\\ &\quad - \frac{a_1(t)\left[1 - \frac{m(t)}{1+n(t)e^{w_1}}\right]e^{w_3}}{1 + b_1(t)e^{w_1}\left[1 - \frac{m(t)}{1+n(t)e^{w_1}}\right] + b_2(t)e^{w_2} + c(t)e^{w_3}}\\ &\equiv F_1(t,w)\\ \frac{dw_2}{dt} &= \frac{\beta(t)e^{w_1}}{1 + be^{w_2}} - d_1(t) - \alpha(t)\\ &\quad - \frac{a_2(t)e^{w_3}}{1 + b_1(t)e^{w_1}\left[1 - \frac{m(t)}{1+n(t)e^{w_1}}\right] + b_2(t)e^{w_2} + c(t)e^{w_3}}\\ &\equiv F_2(t,w)\\ \frac{dw_3}{dt} &= -d_2(t)\\ &\quad + \frac{k_1(t)a_1(t)e^{w_1}\left[1 - \frac{m(t)}{1+n(t)e^{w_1}}\right] + k_2(t)a_2(t)e^{w_2}}{1 + b_1(t)e^{w_1}\left[1 - \frac{m(t)}{1+n(t)e^{w_1}}\right] + b_2(t)e^{w_2} + c(t)e^{w_3}}\\ &\equiv F_3(t,w)\end{aligned} \tag{7}$$

Next, we introduce the spaces

$$\begin{aligned}X = Y = \{w(t) =& (w_1(t), w_2(t), w_3(t))^T \in\\ & C(\mathbb{R}, \mathbb{R}^3) : w(t+\omega) = w(t)\}\end{aligned}$$

equipped with the norm

$$\|w\| = \sum_{i=1}^{3} \max_{t\in[0,\omega]} |w_i(t)|,$$

then X and Y are Banach spaces. Define the linear operator $U : \text{Dom } U \subset X \to Y$ and the continuous mapping $V : X \to Y$ by:

$$Vw = \frac{dw}{dt}, \quad Vw = \begin{pmatrix} F_1(t,w) \\ F_2(t,w) \\ F_3(t,w)\end{pmatrix}.$$

The kernels and images map as:

$$\ker V = \mathbb{R}^3, \quad \text{Im } V = \left\{ v \in Y : \int_0^\omega v(t)dt = 0 \right\}$$

Since Im U is closed in Y and $\dim \ker U = \text{codimIm } U = 3$, U is a Fredholm operator of index zero. The continuous projection operators $S : X \to \ker U$ and $T : Y \to Y/\text{Im } U$ as the averaging operators:

$$Sw = \frac{1}{\omega}\int_0^\omega w(t)dt, \quad Tw = \frac{1}{\omega}\int_0^\omega w(t)dt.$$

Let the inverse of U be defined as $W_S : \text{Im } U \to \ker S \cap \text{Dom } U$, we next show that U is L-compact. By simple computation

$$W_S(w) = \int_0^t w(s)ds - \frac{1}{\omega}\int_0^\omega \int_0^t w(s)dsdt.$$

For any $w(t) \in X$, we have

$$TV(t,w) = \begin{pmatrix} \frac{1}{\omega}\int_0^\omega F_1(t,w)dt \\ \frac{1}{\omega}\int_0^\omega F_2(t,w)dt \\ \frac{1}{\omega}\int_0^\omega F_3(t,w)dt \end{pmatrix},$$

and

$$W_S(I-T)V(t,w) = \begin{pmatrix} \Pi_1 \\ \Pi_2 \\ \Pi_3 \end{pmatrix}$$

where

$$\Pi_i(t) = \int_0^t F_i(t,w)ds - \int_0^\omega \left(1 - \frac{s}{\omega}\right) F_i(t,w)ds - \left(\frac{t}{\omega} - \frac{1}{2}\right)\int_0^\omega F_i(t,w)ds,$$

with $i = 1, 2, 3$.

We will now show that operator V is L-compact on a bounded set $\bar{\Omega} \subset X$ by proving that the sequence of functions generated by the generalized inverse, $W_S(I-T)V(t,w) = (\Pi_1(t), \Pi_2(t), \Pi_3(t))^T$, is both uniformly bounded and equicontinuous. Let $\Omega = \{w \in X : \|w\| < M^*\}$ be an open bounded set, where $M^* > 0$. For any $w(t) = (w_1(t), w_2(t), w_3(t))^T \in \overline{\Omega}$, $\exists\ \tau > 0$ such that $\max_{t\in[0,\omega]} |w_i(t)| \leq \tau$, $i \in \{1,2,3\}$. Since $e^{-\tau} \leq e^{w_1}, e^{w_2}, e^{w_3} \leq e^{\tau}$, and the complex Beddington–DeAngelis fractions are globally bounded by their saturating denominators, we define the maximum values over the periodic domain:

$$|F_1(t,w)| \leq r^M \left(1 + \frac{2e^\tau}{K^L}\right) + \beta^M e^\tau + a_1^M e^q := \delta_1$$
$$|F_2(t,w)| \leq \beta^M e^\tau + d_1^M + \alpha^M + a_2^M e^\tau := \delta_2$$
$$|F_3(t,w)| \leq k_1^M a_1^M e^\tau + k_2^M a_2^M e^\tau + d_2^M := \delta_3.$$

Taking the absolute value of $\Pi_i(t)$ and applying the triangle inequality gives

$$\begin{aligned} |\Pi_i(t)| &\leq \int_0^t |F_i(s,w)|ds \\ &\quad + \frac{1}{\omega}\int_0^\omega \int_0^t |F_i(s,w)|dsdt \\ &\leq \delta_i\omega + \frac{1}{\omega}\left(\delta_i\omega^2\right) = 2\delta_i\omega. \end{aligned}$$

Therefore, the family of functions $\{\Pi_i(t)\}$ is uniformly bounded. To equicontinuity, let $i \in \{1,2,3\}$, then

$$\Pi_i(t_1) - \Pi_i(t_2) = \int_{t_2}^{t_1} F_i(s,w)ds.$$

Taking the absolute value gives

$$\begin{aligned} |\Pi_i(t_1) - \Pi_i(t_2)| &= \left|\int_{t_2}^{t_1} F_i(s,w)ds\right| \\ &\leq \left|\int_{t_2}^{t_1} |F_i(s,w)|ds\right|. \end{aligned}$$

Using our previously defined boundary parameters δ_i, this simplifies to

$$|\Pi_i(t_1) - \Pi_i(t_2)| \leq \delta_i|t_1 - t_2|.$$

Choosing $\delta = \frac{\epsilon}{\max\{\delta_1,\delta_2,\delta_3\}}$ whenever $|t_1 - t_2| < \delta$, gives

$$|\Pi_i(t_1) - \Pi_i(t_2)| \leq \delta|t_1 - t_2| < \delta\left(\frac{\epsilon}{\delta}\right) = \epsilon.$$

Hence, the family of functions $\{\Pi_i(t)\}$ is equicontinuous. By the Arzelá Ascoli Theorem V is L-compact on $\overline{\Omega}$.

We now state the necessary lemmas and theorem required for this work.

Lemma 1. [29] Let $A(t)$, $B(t)$, and $C(t)$ be strictly positive solutions to system (1). If a population satisfies a differential inequality of the form $\dot{y}(t) \leq y(t)(b - ay(t))$ where $a, b > 0$, then

$$y(t) \leq \frac{b}{a}\left[1 + \left(\frac{b}{ay(t_0)} - 1\right)e^{-b(t-t_0)}\right]^{-1}.$$

Lemma 2. [28] If a function $g(t)$ on $[t_0, +\infty)$, and there exists a number $L < +\infty$ such that $\lim_{t\to\infty} g(t) = L$, then $g(t)$ is bounded on $[t_0, +\infty)$.

Mawhin's Continuation Theorem, which serves as the primary mathematical tool for establishing the existence of a positive periodic solution, is stated as follows

Theorem 1. (Mawhin's Coincidence theorem [31]) Let $U : \text{Dom}\, U \subset X \to Y$ be a Fredholm operator of index zero, X and Y Banach spaces, $\Omega \subset X$ an open bounded set and $V : \overline{\Omega} \to Y$ is L-compact on $\overline{\Omega}$. If the following conditions hold:

(i) $Uz = \lambda Vz$, for $z \in \partial\Omega \cap \text{Dom}\, U$, $\lambda \in [0, 1]$;

(ii) $Vz \notin \text{Im}\, U$, $z \in \partial\Omega \cap \ker U$;

(iii) $\deg\{JTV, \Omega \cap \ker U, 0\} \neq 0$, where $J : \text{Im}\, T \to \ker U$ is an isomorphism,

then the equation $Uz = Vz$ has at least one solution on $\bar{\Omega} \cap \text{Dom}\, U$.

Before applying Theorem 1, we establish an a priori bounds for the system $Uw = \lambda Vw$ over $\lambda \in (0, 1)$.

Lemma 3. Consider the system of equations

$$\begin{aligned}
\frac{dA}{dt} &= \lambda\Bigg[\frac{r(t)A}{1+f(t)C}\left(1-\frac{A+B}{K(t)}\right)-\frac{\beta(t)AB}{1+bB}\Bigg] \\
&- \frac{a_1(t)\left[A-R(t,A)\right]C}{1+b_1(t)\left[A-R(t,A)\right]+b_2(t)C+c(t)C}, \\
\frac{dB}{dt} &= \lambda\Bigg[\frac{\beta(t)AB}{1+bB}-d_1(t)B-\alpha(t)B \\
&- \frac{a_2(t)BC}{1+b_1(t)\left[A-R(t,A)\right]+b_2(t)B+c(t)C}\Bigg] \\
\frac{dC}{dt} &= \lambda\Bigg[-d_2(t)C \\
&+ \frac{k_1(t)a_1(t)\left[A-R(t,A)\right]C+k_2(t)a_2(t)BC}{1+b_1(t)\left[A-R(t,A)\right]+b_2(t)B+c(t)C}\Bigg]
\end{aligned} \tag{8}$$

subject to the boundary condition $A(0) > 0$, $B(0) > 0$, $C(0) > 0$. For any $\lambda \in (0, 1)$, and periodic solution (A, B, C) if the following conditions

(H_1) $r^L > \frac{\beta^M E_3}{1+bE_3} + \frac{a_1^M E_5}{1+b_1^L K_2(1-m^M)+b_2^L E_4+c^L E_6} + \frac{r^M E_3}{K^L(1+f^L E_5)}$,

(H_2) $\frac{\beta^L E_2}{1+bE_3} > a_2^M E_5 + \left(d_1^M + \alpha^M\right)$

are satisfied, there exists positive numbers $E_i, (i = 1, 2, \ldots, 6)$ such that $E_2 \leq A(t) \leq E_1$, $E_4 \leq B(t) \leq E_3$, $E_6 \leq C(t) \leq E_5$.

Proof. We will begin the proof by computing the upper bounds E_1, E_3, E_5. From the first equation of system (1), dropping the negative disease and predation terms yields:

$$\begin{aligned}
\frac{dA}{dt} &\leq \lambda\frac{r(t)A}{1+f(t)C}\left(1-\frac{A+B}{K(t)}\right) \\
&\leq \lambda r(t)A\left(1-\frac{A}{K(t)}\right) \\
&\leq \lambda A\left(r^M-\frac{r^L}{K^M}A\right).
\end{aligned}$$

Using Lemma 1 gives

$$A(t) \leq \frac{K^M r^M}{r^L}\left[1+\left(\frac{K^M r^M}{r^L A(t_0)}-1\right)e^{-r^M(t-t_0)}\right]^{-1}$$

while taking the limit as $t \to +\infty$ gives

$$\begin{aligned}
&\lim_{t\to+\infty}\frac{K^M r^M}{r^L}\left[1+\left(\frac{K^M r^M}{r^L A(t_0)}-1\right)e^{-r^M(t-t_0)}\right]^{-1} \\
&= \frac{K^M r^M}{r^L} < \infty.
\end{aligned}$$

By Lemma 2, we obtain

$$A(t) \leq \frac{K^M r^M}{r^L} := E_1.$$

From the second equation, using the identity $1+bB \geq bB$, the transmission term simplifies to $\frac{\beta(t)AB}{1+bB} \leq \frac{\beta(t)A}{b} \leq \frac{\beta^M E_1}{b}$, we have

$$\frac{dB}{dt} \leq \lambda\left[\frac{\beta^M E_1}{b}-\left(d_1^L+\alpha^L\right)B\right]$$

Integrating both sides and applying Lemma 2 gives

$$B(t) \leq \frac{\beta^M E_1}{b\left(d_1^L+\alpha^L\right)} := E_3.$$

For the third equation, we bound the fractions by retaining only the $c(t)C$ term in the denominators (since $\frac{X\cdot C}{Y+c^L C} \leq \frac{X\cdot C}{c^L C} = \frac{X}{c^L}$): $\frac{k_1(t)a_1(t)[A-R(t,A)]C}{1+b_1(t)[A-R(t,A)]+b_2(t)B+c(t)C} \leq \frac{k_1^M a_1^M E_1}{c^L}$ $\frac{k_2(t)a_2(t)BC}{1+b_1(t)[A-R(t,A)]+b_2(t)B+c(t)C} \leq \frac{k_2^M a_2^M E_3}{c^L}$ Substituting these into the $\frac{dC}{dt}$ equation gives: $\frac{dC}{dt} \leq \lambda\left[\frac{k_1^M a_1^M E_1+k_2^M a_2^M E_3}{c^L}-d_2^L C\right]$ By Lemma 1, this provides the upper bound as $C(t) \leq \frac{k_1^M a_1^M E_1+k_2^M a_2^M E_3}{c^L d_2^L} := E_5$ Next, we compute the lower bounds. Using the upper bounds $B(t) \leq E_3$ and $C(t) \leq E_5$, we isolate a lower bound for the first equation

$$\begin{aligned}
\frac{dA}{dt} &\geq \lambda A\Bigg[\frac{r^L}{1+f^M E_5}\left(1-\frac{E_3}{K^L}\right)-\beta^M E_3 \\
&- a_1^M E_5 - \frac{r^M}{K^L(1+f^L E_5)}A\Bigg].
\end{aligned}$$

Setting $g = \frac{r^L}{1+f^M E_5}\left(1-\frac{E_3}{K^L}\right) - \beta^M E_3 - a_1^M E_5$, and assuming the model parameter constraint (H_1) ensures $g > 0$, Lemma (1) yields

$$A(t) \geq \frac{K^L(1+f^L E_5)g}{r^M} := E_2.$$

Minimizing the growth components in the second equation gives

$$\frac{dB}{dt} \geq \lambda B\left[\frac{\beta^L E_2}{1+bE_3} - \frac{a_2^M E_5}{1} - (d_1^M + \alpha^M)\right].$$

Setting $h = \frac{\beta^L E_2}{1+bE_3} - a_2^M E_5 - (d_1^M + \alpha^M)$, constraint (H_2) requires $h > 0$, leading to the lower threshold via Lemma (2)

$$B(t) \geq \min\left\{\frac{h}{2(d_1^M+\alpha^M)},\, B(0)e^{-(d_1^M+\alpha^M)t_1}\right\} := E_4.$$

Finally, note that $A - R(t,A) = A\left(1-\frac{m(t)}{1+n(t)A}\right) \geq E_2(1-m^M)$, hence,

$$\frac{dC}{dt} \geq \lambda C\left[\frac{k_1^L a_1^L E_2(1-m^M) + k_2^L a_2^L E_4}{1+b_1^M E_1 + b_2^M E_3 + c^M E_5} - d_2^M\right].$$

Setting j as the bracketed growth rate constant, then,

$$C(t) \geq \min\left\{\frac{j}{2d_2^M},\, C(0)e^{-d_2^M t_2}\right\} := E_6.$$

□

We now establish the existence of positive periodic solution for the system (1).

Theorem 2. There exists at least one ω-periodic solution for the system (1), if (H_1) and (H_2) holds.

Proof. From Lemma 3, any ω-periodic solution $(A(t), B(t), C(t))^T$ of system (8) for $\lambda \in (0,1)$ satisfies

$$E_2 \leq A(t) \leq E_1, \quad E_4 \leq B(t) \leq E_3,$$
$$E_6 \leq C(t) \leq E_5.$$

Applying logarithmic transformation $w_1(t) = \ln A(t)$, $w_2(t) = \ln B(t)$, and $w_3(t) = \ln C(t)$, these bounds becomes

$$\ln E_2 \leq w_1(t) \leq \ln E_1, \quad \ln E_4 \leq w_2(t) \leq \ln E_3,$$
$$\ln E_6 \leq w_3(t) \leq \ln E_5.$$

A sufficiently large positive constant $M > 0$ is choose such that

$$M > \max_{i=1,\ldots,6}\{|\ln E_i|\}.$$

Next, for $w(t) = (w_1(t), w_2(t), w_3(t))^T$ we define the open bounded set $\Omega \subset X$ as follows

$$\Omega = \{w(t) \in X : \|w\| < M\}.$$

Then, the boundary $\partial\Omega$ satisfies $\|w\| = M$. Therefore, $w \notin \partial\Omega$ for any $w(t)$ a solution to the operator equation $Uw = \lambda Vw$, and $\lambda \in (0,1)$. Thus, condition (i) of Theorem 1 holds. Next, we show that condition (ii) also holds. Let $w \in \partial\Omega \cap \ker U$ such that $Vw \in \text{Im } U$, then $\bar{F}_i(w) = 0$ $(i = 1,2,3)$ where $\bar{F}_i(w) = \frac{1}{\omega}\int_0^\omega F_i(t,w)dt$. By Lemma 3, $\|w\| < M$, which contradicts the assumption that $w \in \partial\Omega$ $(\|w\| = M)$. Hence, $Vw \notin \text{Im } U$ for $w \in \partial\Omega \cap \ker U$ satisfying condition (ii). Finally, We define a continuous topological degree homotopy

$$H(w,\mu) : (\Omega \cap \ker U) \times [0,1] \to \mathbb{R}^3.$$

Using the parameter μ, the decoupled system becomes

$$H_1(w,\mu) = \bar{r}\left(1 - \frac{e^{w_1}+e^{w_2}}{\bar{K}}\right) - \mu\left[\frac{\bar{f}\bar{r}e^{w_3}}{1+\bar{f}e^{w_3}}\left(1 - \frac{e^{w_1}+e^{w_2}}{\bar{K}}\right) + \frac{\bar{\beta}e^{w_2}}{1+be^{w_2}} + \frac{\bar{a}_1(1-\bar{m})e^{w_3}}{D(w)}\right]$$

$$H_2(w,\mu) = \frac{\bar{\beta}e^{w_1}}{1+be^{w_2}} - (\bar{d}_1 + \bar{\alpha}) - \mu\left[\frac{\bar{a}_2 e^{w_3}}{D(w)}\right]$$

$$H_3(w,\mu) = \frac{\alpha\bar{n}e^{w_1}}{(1+k_1e^{w_1})(1+k_2e^{w_3})} - \bar{d}_2 + \mu\left[\frac{\bar{k}_{22}e^{w_2} - \alpha\bar{n}e^{w_1}}{D(w)}\right]$$

where $D(w) = 1 + \bar{b}_1(1-\bar{m})e^{w_1} + \bar{b}_2 e^{w_2} + \bar{c}e^{w_3}$. By the homotopy invariance property of topological degree

$$\begin{aligned}
&\deg\{JTV, \Omega\cap\ker U, 0\}\\
&= \deg\{H(w,1), \Omega\cap\ker U, 0\}\\
&= \deg\{H(w,0), \Omega\cap\ker U, 0\}\\
&= \begin{vmatrix} -\frac{\bar{r}e^{w_1^*}}{\bar{K}} & -\frac{\bar{r}e^{w_2^*}}{\bar{K}} & 0\\ \frac{\bar{\beta}e^{w_1^*}}{1+be^{w_2^*}} & -\frac{b\bar{\beta}e^{w_1^*+w_2^*}}{(1+be^{w_2^*})^2} & 0\\ Q_1 & Q_2 & -Q_3 \end{vmatrix}\\
&= \text{sgn}\left[-Q_3\left(\frac{b\bar{r}\bar{\beta}e^{2w_1^*+w_2^*}}{\bar{K}(1+be^{w_2^*})^2} + \frac{\bar{r}\bar{\beta}e^{w_1^*+w_2^*}}{\bar{K}(1+be^{w_2^*})}\right)\right]\\
&= -1 \neq 0,
\end{aligned}$$

where $Q_3 = \frac{\bar{d}\bar{c}e^{w_2^*}}{D} > 0$. Condition (iii) is also satisfied. Since all the conditions of Theorem 1 are satisfied, the system 1 has at least one ω-periodic solution. □

5 Global Stability and Uniqueness of Solution

In this section we will investigate the global stability of system (1). We will first state a required definition and lemma.

Definition 1. [30] The positive ω-periodic solution vector $(\tilde{A}(t), \tilde{B}(t), \tilde{C}(t))^T$ is called a global attractor of the system (1) if for any other arbitrary positive solution trajectory $(A(t), B(t), C(t))^T$ evaluated in $\mathbb{R}^3_+$, the following limits holds

$$\lim_{t\to\infty} |A(t) - \tilde{A}(t)| = 0, \quad \lim_{t\to\infty} |B(t) - \tilde{B}(t)| = 0,$$
$$\lim_{t\to\infty} |C(t) - \tilde{C}(t)| = 0.$$

Lemma 4. [28, 30] If a non-negative functions g is integrable and uniformly continuous on $[0, +\infty)$, then $\lim_{t\to\infty} g(t) = 0$.

Let $w(t) = (w_1(t), w_2(t), w_3(t))^T$ and $\tilde{w}(t) = (\tilde{w}_1(t), \tilde{w}_2(t), \tilde{w}_3(t))^T$ be any two positive ω-periodic solutions to the operator equation $Uw = Nw$. We define a non-negative, global logarithmic Lyapunov functional

$$V(t) = |w_1(t) - \tilde{w}_1(t)| + |w_2(t) - \tilde{w}_2(t)| + |w_3(t) - \tilde{w}_3(t)|.$$

The upper right Dini derivative $D^+V(t)$ of the non-autonomous system is

$$D^+V(t) = \sum_{i=1}^{3} \text{sgn}\,(w_i(t) - \tilde{w}_i(t)) \cdot [F_i(t, w) - F_i(t, \tilde{w})] \tag{9}$$

where

$$\text{sgn}\,(w_1 - \tilde{w}_1)(F_1(t, w) - F_1(t, \tilde{w})) \leq -\frac{r(t)}{(1 + f(t)e^{w_3})K(t)}|A - \tilde{A}| + \beta(t)|B - \tilde{B}| + \Gamma_1|C - \tilde{C}|, \tag{10}$$

$$\text{sgn}\,(w_2 - \tilde{w}_2)(F_2(t, w) - F_2(t, \tilde{w})) \leq \beta(t)|A - \tilde{A}| - \frac{b\beta(t)e^{w_1}}{(1 + be^{w_2})^2}|B - \tilde{B}| + \Gamma_2|C - \tilde{C}|, \tag{11}$$

and

$$\text{sgn}\,(w_3 - \tilde{w}_3)(F_3(t, w) - F_3(t, \tilde{w})) \leq \bar{k}_1 a_1(t)|A - \tilde{A}| + \bar{k}_2 a_2(t)|B - \tilde{B}| - \frac{d_2(t)c(t)e^{w_3}}{D(w)D(\tilde{w})}|C - \tilde{C}|. \tag{12}$$

Substituting, (10), (11) and (12) into (9) gives

$$D^+V(t) \leq -L_1(t)|A(t) - \tilde{A}(t)| - L_2(t)|B(t) - \tilde{B}(t)| - L_3(t)|C(t) - \tilde{C}(t)|$$

where

$$L_1(t) = \frac{r^L}{(1 + f^M Z_3)K^M} - \beta^M - \bar{k}_1 a_1^M > 0,$$

$$L_2(t) = \frac{b\beta^L E_2}{(1 + bE_3)^2} - \beta^M - \bar{k}_2 a_2^M > 0,$$

$L_3(t) = \dfrac{d_2^L c^L E_6}{\max(D^2)} - \Gamma_1 - \Gamma_2 > 0$. For L_i, $(i = 1, 2, 3)$, there exist positive constants $\delta_1, \delta_2, \delta_3 > 0$ such that

$$D^+V(t) \leq -\delta_1|A(t) - \tilde{A}(t)| - \delta_2|B(t) - \tilde{B}(t)| - \delta_3|C(t) - \tilde{C}(t)|, \quad \forall t \geq T_2$$

Integrating this from T_2 to t yields

$$V(t) + \int_{T_2}^{t} (\delta_1|A(\tau) - \tilde{A}(\tau)| + \delta_2|B(\tau) - \tilde{B}(\tau)| + \delta_3|C(\tau) - \tilde{C}(\tau)|)d\tau \leq V(T_2) < \infty. \tag{13}$$

By Lemma 4, we get

$$\lim_{t\to\infty} |A(t) - (t)| = 0, \quad \lim_{t\to\infty} |B(t) - B(t)| = 0,$$
$$\lim_{t\to\infty} |C(t) - C(t)| = 0. \tag{14}$$

Hence, the positive ω-periodic solution of the system $Uw = Nw$ is globally asymptotically stable. We now prove that the solution is unique. Suppose there exist two distinct positive ω-periodic solutions to the operator system $Uw = Nw$, which denoted by $w^*(t) = (w_1^*(t), w_2^*(t), w_3^*(t))^T$ and $w^-(t) = (w_1^-(t), w_2^-(t), w_3^-(t))^T$, reversing the logarithmic transformation gives $(A^*(t), B^*(t), C^*(t))^T$ and $(A^-(t), B^-(t), C^-(t))^T$ for all $t \in [0, \omega]$. There exist at least one time point $\xi \in [0, \omega]$ such that $A^*(\xi) \neq A^-(\xi)$. Also,

$$|A^*(\xi) - A^-(\xi)| = \delta_A > 0.$$

Therefore, for any non-negative integer $q \in \mathbb{N}$,

$$\lim_{q\to+\infty} |A^*(\xi + q\omega) - A^-(\xi + q\omega)| = \lim_{t\to+\infty} |A^*(t) - A^-(t)| = \delta_A > 0$$

This contradicts (14). Hence, $A^*(t) \equiv A^-(t)$, $B^*(t) \equiv B^-(t)$ and $C^*(t) \equiv C^-(t)$, $\forall t \in [0, \omega]$. Thus, the system $Uw = Nw$ possesses exactly one unique positive ω-periodic solution.

6 Numerical Simulation

In this section, we run numerical simulations to validate our analytic results visually. The following parameter set will be used for the numerical simulation ($r = 1.2$, $K = 100.0$, $\beta = 0.4$, $b = 0.05$, $m = 0.3$, $n = 0.1$, $a_1 = 0.5$, $a_2 = 0.7$, $b_1 = 0.2$, $b_2 = 0.1$, $c = 0.05$, $k_1 = 0.4$, $k_2 = 0.5$, $d_1 = 0.1$, $d_2 = 0.2$, $\alpha = 0.2$, $f = 0.2$). The long-term behaviour of the population of the ecosystem is shown in Figure 2 Appendix A. Figure 2(a)-(c) Appendix A is the time-series trajectories for the susceptible prey $A(t)$, infected prey $B(t)$, and predator $C(t)$ populations, respectively. It is evident that the independent solution trajectories rapidly converge across seasonal cycles, which strongly supports our analytical criteria for a global asymptotic attractor. Figure 2(d) Appendix A shows the corresponding three-dimensional phase portrait. Irrespective of the initial starting configurations, all solution lines align into a single, well-defined closed-loop trajectory, confirming that the system possesses a unique positive ω-periodic solution.

Next, the ecological consequences of varying the indirect predator-induced fear factor $f(t)$ on the ecosystem is examined using three different fear intensities, low fear intensity ($f = 0.05$), moderate fear intensity ($f = 0.50$), and high fear intensity, ($f = 2.50$). The resulting temporal patterns are presented in Figure 3 Appendix A. As the intensity of the prey refuge increases from low to high, the birth rate of the susceptible prey is significantly suppressed, leading to a visible drop in the healthy prey population density. Outbreak of disease in the ecosystem is weakened. As the population of the available healthy and infected prey decreases, the predator population experiences a secondary resource limitation, resulting in lower predator densities due to food scarcity. In Figure 3(d) Appendix A increasing the fear factor causes the periodic attractors to physically shift positions and contract in volume, demonstrating a strong behavioral regulation over the spatial scale of the stable cycles.

Figure 4 Appendix A shows the behaviour of the different population at various disease transmission rate. At low transmission rates, the infection cannot be sustained, causing the disease to die out completely. In this state, the susceptible prey does not lose any portion of its population to infection. However, as the disease transmission rate increases, the steady-state population of susceptible prey drops due to increased disease vulnerability. Conversely, higher transmission rates fuel an increase in the infected prey population, which simultaneously drives up the predator population density due to the availability of weaker, easily exploitable infected prey.

The impact of the saturating prey refuge function $R(t, A)$ is visualized in Figure 1 Appendix A. Protecting a portion of healthy prey affects the encounter rates governed by the Beddington–DeAngelis functional response. The simulations show that optimal refuge allocations protect the core breeding stock of susceptible prey from over-exploitation, which determines whether the eco-epidemiological subpopulations settle into stable periodic coexistence or undergo radical structural shifts.

7 Conclusion

In this paper, we considered a non-autonomous, three-dimensional predator-prey eco-epidemiological model incorporating disease transmission, a predator-induced fear on susceptible prey, a saturating prey refuge, and a Beddington–DeAngelis functional response. we initially established the well-posedness of the system dynamics within a compact invariant region. By utilizing Mawhin's Coincidence Theorem and a logarithmic coordinate transformation, we derived sufficient analytical conditions ensuring the existence of at least one positive ω-periodic solution. Furthermore, by constructing a global logarithmic Lyapunov functional, we established the exact conditions under which this periodic solution acts as a unique global attractor for the entire ecosystem. Numerical simulations were used to validate our analytic results. This study demonstrates that incorporating indirect behavioral costs, structural refuges, and seasonal fluctuations yields a more comprehensive representation of wildlife epidemics and predator-prey dynamics. The authors are grateful to the anonimous reviewers

References:

[1] L. Y. Zanette, A. F. White, M. C. Allen, and M. Clinchy, "Perceived predation risk reduces the number of offspring songbirds produce per year," Science vol. 334 , no. 6061, pp. 1398–1401, 2011. https://doi.org/10.1126/science.1210908.

[2] X. Wang, L. Zanette, and X. Zou. "Modelling the fear effect in predator–prey interactions," J. Math. Biol. vol. 73 no. 5, 1179–1204, 2016, https://doi.org/10.1126/science.1210908.

[3] K. Wang, L. Zanette, and X. Zou."Modelling the fear effect in predator–prey interactions," J. Math. Biol. vol. 73, pp. 1179–1204, 2016, https://doi.org/10.1007/s00285-016-0989-1.

[4] A. Das, and G. P. Samanta. "Modeling the fear effect on a stochastic prey–predator system with

additional food for the predator," Journal of Physics A: Mathematical and Theoretical vol. 51, iss. 46, 2018: 465601.

[5] P. Panday, N. Pal, S. Samanta, and J. Chattopadhyay. "Stability and bifurcation analysis of a three-species food chain model with fear," Int. J. Bifurcation Chaos, vol. 28 , no. 1, 1850009, 2018, https://doi.org/10.1142/S0218127418500098.

[6] B. Dubey , S. Sajan , A. Kumar. "Stability switching and chaos in a multiple delayed prey-predator model with fear effect and anti-predator behavior," Math. Comput. Simul.vol. 188, pp. 164–192, 2021. https://doi.org/10.1016/j.matcom.2021.03.037.

[7] X. Wang, and X. Zou. "Modeling the Fear Effect in Predator-Prey Interactions with Adaptive Avoidance of Predators," Bull Math Biol. vol. 79, pp. 1325-1359, 2017. doi: 10.1007/s11538-017-0287-0.

[8] S. Halder, J. Bhattacharyya, and S. Pal. "Predator-prey interactions under fear effect and multiple foraging strategies," Discrete Contin. Dyn. Syst. Ser. B, vol. 2, pp. 3779, 2022. https://doi.org/10.3934/dcdsb.2021206.

[9] N. Bairagi, S. Chaudhuri, and J. Chattopadhyay. "Harvesting as a disease control measure in an eco-epidemiological system – A theoretical study," Math. Biosci. vol. 217, iss. 2, pp. 134-144, 2009, https://doi.org/10.1016/j.mbs.2008.11.002.

[10] I. Siekmann, H. Malchow, and E. Venturino. "On competition of predators and prey infection, Ecological Complexity," vol. 7, Iss. 4, pp. 446-457, 2010. https://doi.org/10.1016/j.ecocom.2009.10.005.

[11] E. Venturino. "Epidemics in predator-prey models: Disease in the predators," IMA J. Math. Appl. Med. Biol., 2002. https://doi.org/10.1093/imammb/19.3.185 doi: 10.1093/imammb/19.3.185

[12] M. Haque. "A predator-prey model with disease in the predator species only," Nonlinear Anal. Real., 2010. https://doi.org/10.1016/j.nonrwa.2009.06.012 doi: 10.1016/j.nonrwa.2009.06.012

[13] E. Francomano, M. F. Hilker, M. Paliaga, and E. Venturino. "Diseased social predators," Bull. Math. Biol., 2017. https://doi.org/10.1007/s11538-017-0325-y doi: 10.1007/s11538-017-0325-y

[14] S. Sarwardi, M. Haque, and E. Venturino. "Global stability and persistence in LG-Holling type II diseased predator ecosystems," J. Biol. Phys., 2011. https://doi.org/10.1007/s10867-010-9201-9 doi: 10.1007/s10867-010-9201-9

[15] A. A. Shaikh, H. Das, and N. Ali. "Study of LG-Holling type III predator-prey model with disease in predator," J. Appl. Math. Comput., 2017. https://doi.org/10.1007/s12190-017-1142-z doi: 10.1007/s12190-017-1142-z

[16] A. Sha, and J. Chattopadhyay. "Dynamical study of fear effect in prey-predator model with disease in predator," Journal of Biological Systems, vol. 31, pp. 1319-1340, 2023. https://doi.org/10.1142/S0218339023500444

[17] K. D. Lafferty, and A, K. Morris, "Altered behavior of parasitized killifish increases susceptibility to predation by bird final hosts," Ecology, vol. 77, iss. 5, pp. 1390–1397, 1996. https://doi.org/10.2307/2265536

[18] J. Wang, Y. Cai, S. Fu, and W. Wang. "The effect of the fear factor on the dynamics of a predator-prey model incorporating the prey refuge. Chaos 29, 2019. https://doi.org/10.1063/1.5111121

[19] A. Das, and G.P. Samanta. "A prey–predator model with refuge for prey and additional food for predator in a fluctuating environment," Physica A vol. 538 pp. 427–450, 2019. https://doi.org/10.1016/j.physa.2019.122844

[20] G. Tang, S. Tang, and R. A. Cheke, "Global analysis of a Holling type II predator–prey model with a constant prey refuge," Nonlinear Dyn. vol. 76, iss. 1, pp. 635–647, 2014. https://doi.org/10.1007/s11071-013-1157-4

[21] X. Wang, Y. Tan, Y. Cai, and W. Wang, "Impact of the fear effect on the stability and bifurcation of a Leslie-Gower predator-prey model," Int. J. Bifurcat. Chaos 30, 2020. https://doi.org/10.1142/S0218127420502107

[22] J. P. Tripathi, S. Abbas, and M. Thakur, "A density dependent delayed predator–prey model with Beddington–DeAngelis type function response incorporating a prey refuge," Commun Nonlin- ear Sci. Numer. Simul. vol. 22, iss. 1–3, pp. 427–450, 2015. https://doi.org/10.1016/j.cnsns.2014.08.018

[23] G. A. Polis, and C. A. Myers, "The ecology and evolution of intraguild predation: potential competitors that eat each other," Annual Review of Ecology, Evolution, and Systematics, vol 20, pp. 297-330. https://doi.org/10.1146/annurev.es.20.110189.001501

[24] D. Pal, G.S. Mahaptra, and G.P. Samanta, "Optimal harvesting of prey–predator system with interval biological parameters: a bioeconomic model," Math. Biosci. vol. 241, iss. 2, pp. 181–187, 2013. https://doi.org/10.1016/j.mbs.2012.11.007

[25] N. Sari, and E. A. Véron, "Periodic orbits of a seasonal SIS epidemic model with migration," J. Math. Anal. Appl. vol. 423, pp. 1849–1866, 2015. https://doi.org/10.1016/j.jmaa.2014.10.084.

[26] H. Zheng, L. Guo, Y. Bai, and Y. Xia, "Periodic solutions of a non-autonomous predator-prey system with migrating prey and disease infection: via Mawhin coincidence degree theory," J. Fixed Point Theory Appl. vol. 260, pp. 21–37, 2019. https://doi.org/10.1007/s11784-019-0674-2.

[27] C. M. Silva, "Existence of periodic solutions for periodic eco-epidemic models with disease in the prey," J. Math. Anal. Appl. vol. 453, pp. 383–397, 2017.

[28] K. Gopalasamy, Stability and Oscillation in Delay Equation of Population Dynamics. Kluwer Academic Publishers, Dordrecht (1992)

[29] C. Chen, and F. Chen, "Conditions for global attractivity of multispecies ecological competition-predator system with Holling-type III functional response," J. Biomath. vol. 19, pp. 136–140, 2004. https://api.semanticscholar.org/CorpusID:87881065.

[30] Y. Zhu, and K. Wang, "Existence and global attractivity of positive periodic solutions for a predator–prey model with modified Leslie–Gower Holling-type II schemes," J. Comput. Appl. Math. vol. 384, pp. 408–418, 2011. http://dml.cz/dmlcz/146947.

[31] R. Gaines, and J. Mawhin, Coincidence Degree and Nonlinear Differential Equations. Springer, Berlin (1977).

Contribution of Individual Authors to the Creation of a Scientific Article (Ghostwriting Policy)

The authors equally contributed in the present research, at all stages from the formulation of the problem to the final findings and solution.

Sources of Funding for Research Presented in a Scientific Article or Scientific Article Itself

No funding was received for conducting this study.

Conflicts of Interest

The authors have no conflicts of interest to declare that are relevant to the content of this article.

Creative Commons Attribution License 4.0 (Attribution 4.0 International , CC BY 4.0)

This article is published under the terms of the Creative Commons Attribution License 4.0
https://creativecommons.org/licenses/by/4.0/deed.en_US

A Appendix: Figures

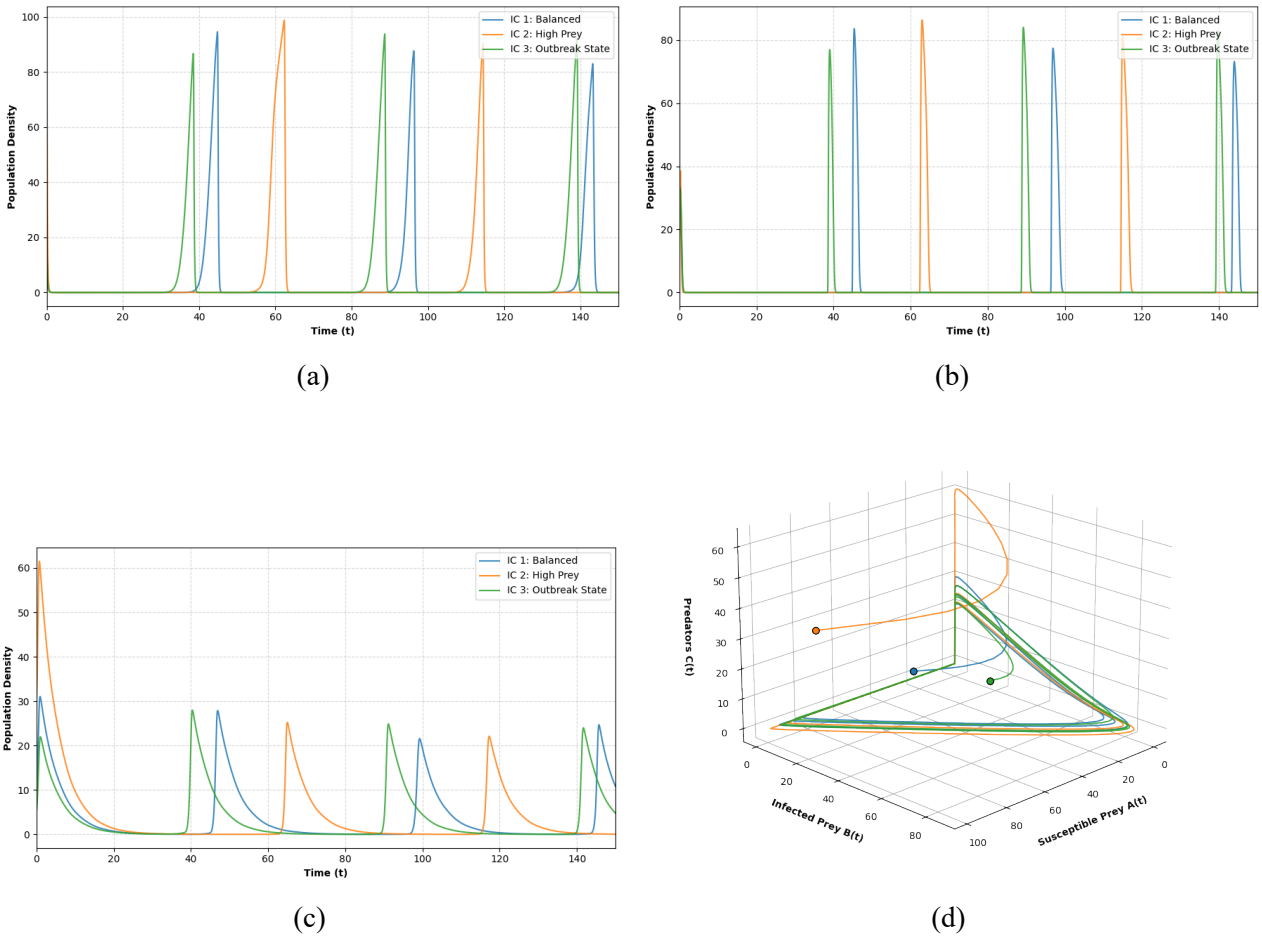

Figure 1: Numerical verification of the global attractivity and uniqueness of the positive periodic solution under baseline parameter values ($r = 1.2, K = 100.0, \beta = 0.4, b = 0.05, m = 0.3, n = 0.1, a_1 = 0.5, a_2 = 0.7, b_1 = 0.2, b_2 = 0.1, c = 0.05, k_1 = 0.4, k_2 = 0.5, d_1 = 0.1, d_2 = 0.2, \alpha = 0.2, f = 0.2$). (a) Time series plot showing synchronization of susceptible prey $A(t)$. (b) Time series plot showing synchronization of infected prey $B(t)$. (c) Time series plot showing synchronization of predator $C(t)$. (d) Three-dimensional phase portrait showing the convergence of all trajectories into a unique closed loop.
Source: Created by the Authors.

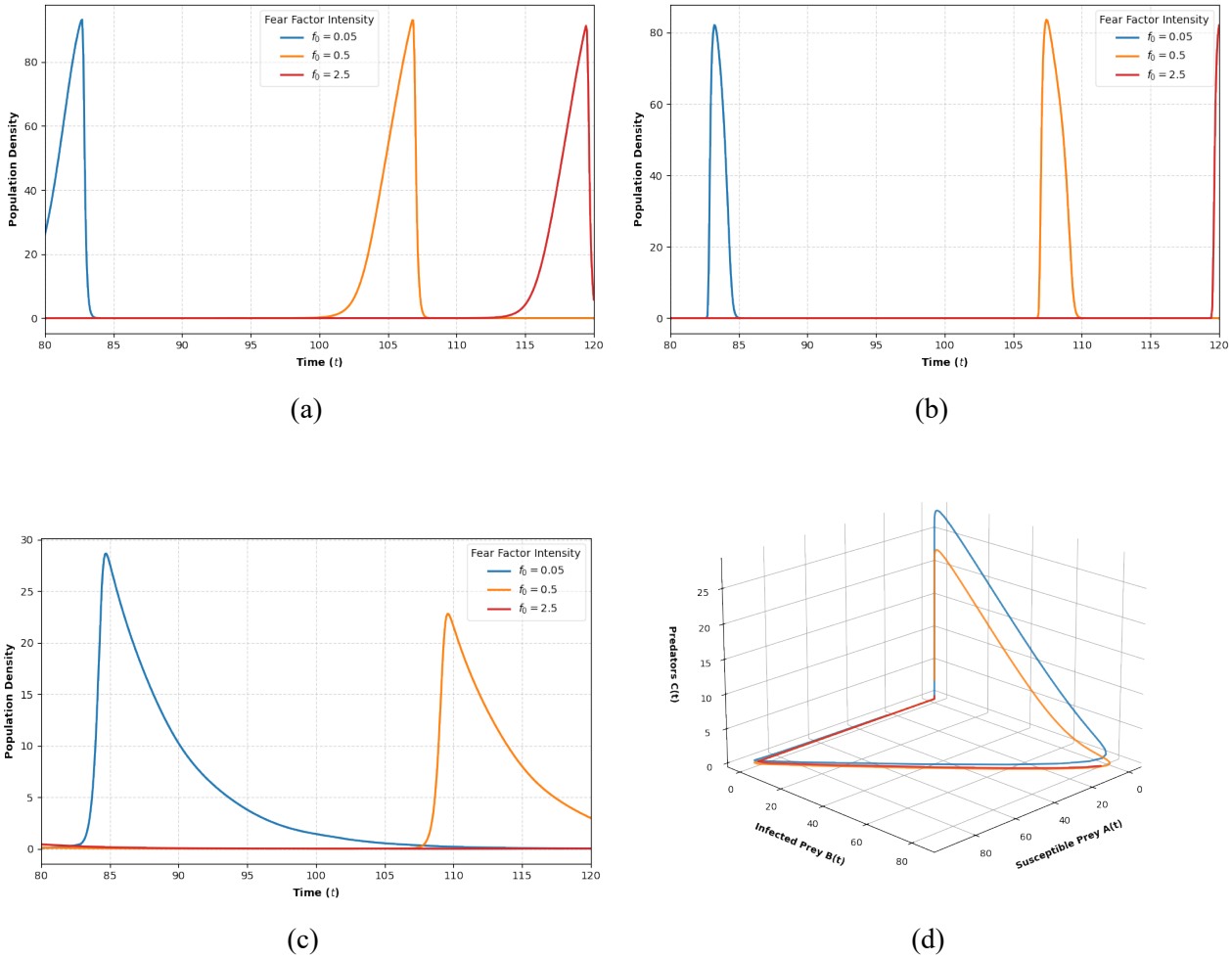

Figure 2: The ecological impacts of varying predator-induced fear intensity ($f = 0.05, 0.50, 2.50$) over time. (a) Suppression of susceptible prey $A(t)$ densities at higher fear levels. (b) Attenuation of the disease outbreak in infected prey $B(t)$ due to suppressed reproduction. (c) Drop in predator $C(t)$ abundance resulting from food scarcity. (d) Phase portrait illustrating the physical shifting and shrinkage of the periodic attractors as fear intensifies.
Source: Created by the Authors.

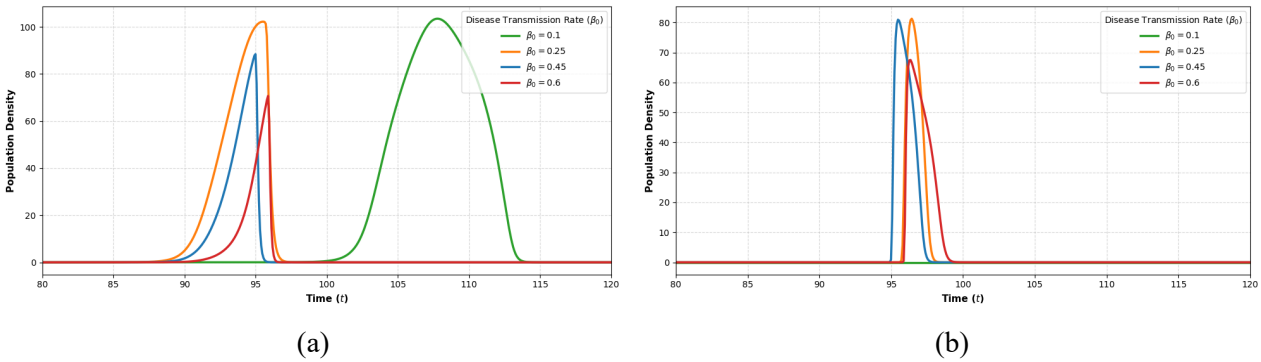

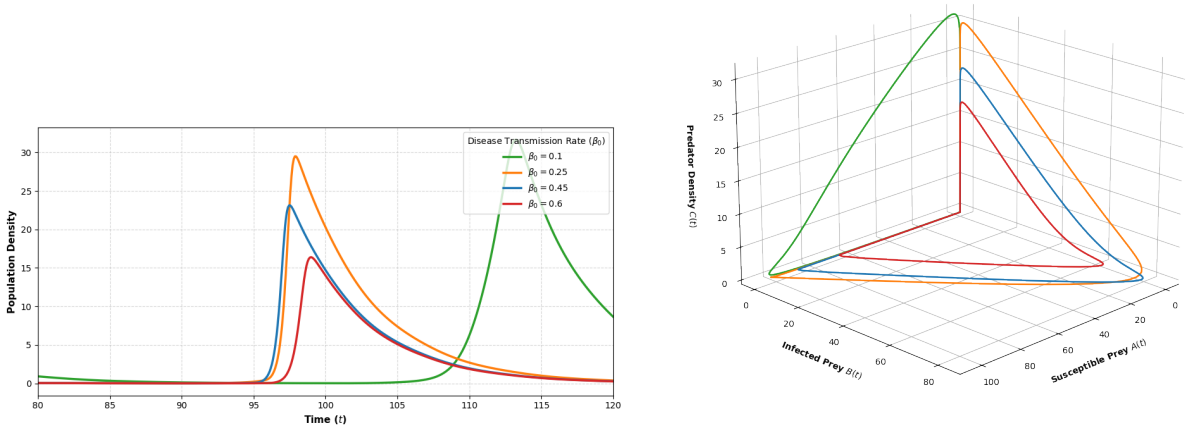

(c) (d)

Figure 3: Dynamic behavior of the ecosystem subpopulations across different disease transmission rates (β). (a) Time series of susceptible prey $A(t)$ illustrating population decline at higher transmission rates. (b) Time series of infected prey $B(t)$ showing epidemic escalation. (c) Time series of predator $C(t)$ depicting population gains driven by infected prey availability. (d) Phase portrait tracking the multi-species structural adjustments under varying infectious forces.
Source: Created by the Authors.

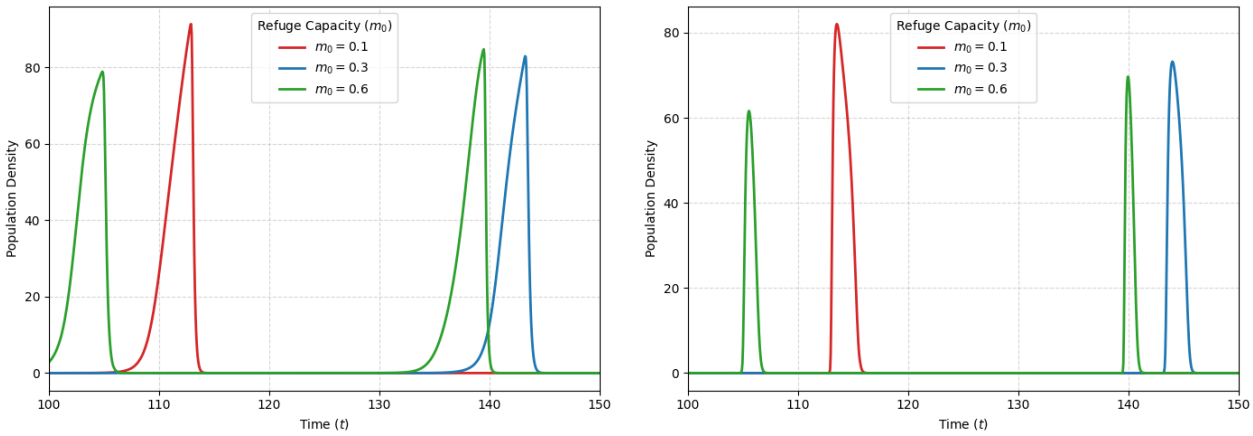

(a) (b)

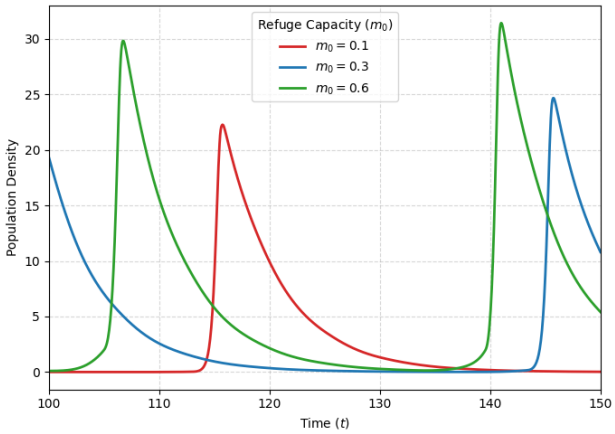

(c)

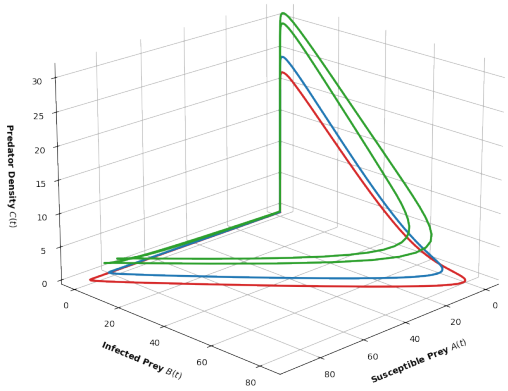

(d)

Figure 4: Influence of alternative refuge capacity coefficients ($m_0 = 0.1, 0.3, 0.6$) on multi-species periodicity. (a) Time series plot of susceptible prey $A(t)$ under varying refuge protections. (b) Time series plot of infected prey $B(t)$ reflecting epidemiological shifts. (c) Time series plot of predator $C(t)$ displaying resource-dependent oscillations. (d) Phase portrait showing the structural convergence of the system trajectories toward stabilized periodic cycles.
Source: Created by the Authors.